Dyes and Pigments 88 (2010) 204–211

Contents lists available at ScienceDirect

Dyes and Pigments

journal homepage: www.elsevier.com/locate/dyepig

The photophysical characterisation of novel 3,9-dialkyloxy- and diacyloxyperylenes

John F. Fuini [a], Anand B. Surampudi [a], Mark A. Penick [b], Mathew P.D. Mahindaratne [b], George R. Negrete [b], Lorenzo Brancaleon [a,*]

[a] Department of Physics and Astronomy, University of Texas at San Antonio, One UTSA Circle, San Antonio, TX 78249, USA
[b] Department of Chemistry, University of Texas at San Antonio, One UTSA Circle, San Antonio, TX 78249, USA

ARTICLE INFO

Article history:
Received 26 March 2010
Received in revised form
17 June 2010
Accepted 20 June 2010
Available online 1 July 2010

Keywords:
Perylene
Photophysics
Solvent interaction
Excited state lifetimes
Quantum efficiency

ABSTRACT

The fundamental photophysical properties of three symmetrically substituted 3,9-perylene analogues were examined in a diverse range of solvents. All three compounds exhibited solvent-dependent fluorescence quantum yield, which was lower than that of perylene or its diimides. Whilst the absence of a large excited state dipole moment suggests that there is no preferential charge accumulation in one side of the molecules, the data suggest that intramolecular electron transfer occurs and that such an event causes additional photochemical mechanisms in chlorinated compounds where the fluorescence quantum yield is lower than in all other solvents and the values of the fluorescence decay change significantly. The dyes could be an interesting new class of fluorescence tags for labeling biomolecules and as dyes for organic photovoltaic materials.

1. Introduction

Perylene and its analogues [1] are an interesting class of polyaromatic hydrocarbons (PAH) that are investigated for diverse applications including organic solar cells [2], fluorescence labeling [3], molecular sensors [4], and molecular electronics [5]. Perylene diimides have been the most studied perylene derivatives [6,7] because of the electron accepting properties of the π-system, which results from the electron-withdrawing carbonyl substituents [8]. The $\pi-\pi^*$ transition in perylene and its substituted analogues has been used as a model for many photophysical studies [9,10], and this work is expanding as new perylene compounds are developed to optimize desirable photophysical properties. Perylene analogues with electron donating groups may provide favorable properties for photoactive dyes [11], but few have appeared in the literature with overall donating substituent effects [12,13].

Recently reported 3,9-dialkyloxy-substituted perylenes [14] provide new examples of unprecented electronic properties (Scheme 1, products **1** and **2**)[14]. Such products are attractive since alkyloxy appendages are expected to stabilize perylene radical cation intermediates resulting in facile charge separation. The previous report addressed their synthesis and the chemical structures but did not examine their photophysics [14]. Here we investigate some of the fundamental photophysical properties of these two perylenes, 3,9-dimethoxyperylene (**1**) and 3,9-bis(1-octyloxy) perylene (**2**), and a new, less electron donating analogue 3,9-bis(1-octanoyloxy)perylene (**3**), which was prepared for these studies. The absorption and emission spectra as well as the fluorescence lifetimes of these three compounds are characterized in various solvents. Parameters such as the molar extinction coefficients (ε) and the fluorescence quantum efficiencies (Φ_f) as a function of solvent are also calculated and compared with those reported (or measured) for the unsubstituted perylene.

2. Experimental

2.1. Chemicals

Perylenes **1** and **2** were synthesized as reported previously [14] by tandem Friedel-Crafts annulation of the corresponding tetrahydronaphthol components **5b** and **5c**, respectively followed by catalytic oxidation (Scheme 1). Novel diester **4d** (R = C(O)-*n*-C_7H_{15}) was made available upon esterification of octahydroperylene-4,10-diol intermediate **4a** (from **5a**) [14] using *n*-octanoyl chloride and was converted to **3** upon chloranil oxidation (Scheme 1). The synthesis and characterization of **3** are described below.

* Corresponding author. Tel.: +1 210 458 5694; fax: +1 210 458 5191.
E-mail address: lorenzo.brancaleon@utsa.edu (L. Brancaleon).

0143-7208/$ – see front matter © 2010 Elsevier Ltd. All rights reserved.
doi:10.1016/j.dyepig.2010.06.009

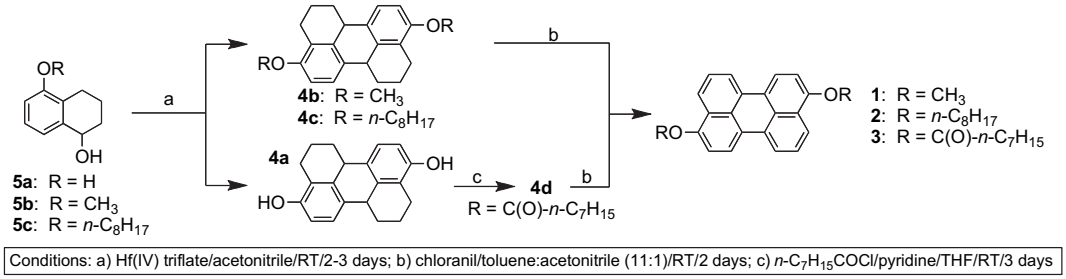

Scheme 1. The general synthetic approach to 3,9-disubstituted perylenes **1**–**3**.

2.2. Solvents

Carbon tetrachloride (CCl_4), toluene, pyridine, chloroform ($CHCl_3$), tetrahydrofuran (THF), and dichloromethane (CH_2Cl_2) were purchased as spectrophotometric grade solvents from Aldrich and used without additional purification. Pyridine and THF were dried using the methods described in Supplemental Information.

2.3. Preparation of 1,2,3,6b,7,8,9,12b-octahydroperylene-4,10-diyl dioctanoate (**4d**, R = C(O)(CH_2)$_6$$CH_3$)

To a flask containing 1,2,3,6b,7,8,9,12b-octahydroperylene-4,10-diol (**4a**, R = H; 400 mg, 1.37 mmol) partially dissolved in THF (5 mL) under N_2 was added excess pyridine (1.0 mL, 12.4 mmol) and octanoyl chloride (0.6 mL, 3.5 mmol) and the deep green reaction mixture was stirred for three days at room temperature. The remaining solid materials of the mixture were filtered out and the filtrate was diluted with CH_2Cl_2 (20 mL). The excess pyridine was removed by washing the organic layer with water (20 mL) and dilute HCl (2 × 22 mL). The organic layer was dried over anhydrous $MgSO_4$, filtered, and the filtrate was mixed with ethyl acetate (30 mL). The solvent was removed to reduce the volume to approximately one fourth by rotary evaporation. A small sample was removed and allowed to dry in a cuvette to provide crystals used to seed the rest of the mixture. The crystal suspension was stirred at room temperature for 1.5 h and at 0 °C for 4 h, then filtered and washed with cold ethyl acetate to obtain product **4d** (R = C(O)(CH_2)$_6$$CH_3$) as a white powder (209 mg, 28%), mp: 140.5–142 °C; ^{1}H NMR (300 MHz, $CDCl_3$): δ 7.28 (d, 2H, J = 9.0 Hz), 6.94 (d, 2H, J = 9.0 Hz), 3.79–3.74 (m, 2H), 2.81–2.75 (m, 2H), 2.59 (t, 4H, J = 8.0 Hz), 2.55 (octet, 2H, J = 4.6 Hz), 2.51–2.43 (m, 2H), 2.11–2.01 (m, 2H), 1.79 (quintet, 4H, J = 7.5 Hz), 1.74–1.65 (m, 2H), 1.59–1.48 (m, 2H), 1.48–1.26 (m, 16H), 0.92–0.88 (m, 6H); ^{13}C NMR (75 MHz, $CDCl_3$): δ 14.2, 20.7, 21.9, 22.7, 25.2, 29.0, 29.2, 29.7, 31.8, 34.4, 36.0, 119.5, 125.0, 130.1, 132.6, 136.7, 145.8, 172.3; MS (m/z): 544.1, 418.1, 292.2; IR (cm^{-1}): 2953, 2923, 2857, 1750, 1482, 1209, 1138, 1118; Exact mass: calc'd for $C_{36}H_{48}O_4$ (M^+), 544.3553. Found, 544.3507.

2.4. Preparation of perylene-3,9-diyl dioctanoate (**3**)

A mixture of 153 mg (0.28 mmol) of **4d** (R = C(O)(CH_2)$_6$$CH_3$) and 7 mL of toluene was stirred until dissolved in a round-bottom flask placed in an ambient temperature water bath. To this clear solution, 2,3-dichloro-5,6-dicyano-1,4-benzoquinone (DDQ; 258 mg, 1.14 mmol) was added and the resultant dark red mixture was allowed to stand for two days after being stirred for one day (note: chloranil, 2,3,5,6-tetrachloro-1,4-benzoquinone, can also be used in place of DDQ in oxidation step and is seemingly the better oxidizing agent for the other octahydroperylene derivatives). A yellow colored precipitate was formed during standing and was collected by filtration. The solid was sequentially crystallized from THF/CH_3CN while monitoring the purity by FT-IR (the CN stretch of reduced DDQ no longer appeared in the IR spectrum of the product after two crystallizations). Compound **3** was obtained as a yellow powder (81 mg, 54%), mp: 150–151 °C; ^{1}H NMR (300 MHz, $CDCl_3$): δ 8.12–8.06, (m, 4H), 7.68 (dd, 2H, J = 8.4, 0.5 Hz), 7.48 (dd, 2H, J = 8.4, 7.5 Hz), 7.42 (d, 2H, J = 8.1 Hz), 2.74 (t, 4H, J = 7.5 Hz), 1.93–1.82 (m, 4H), 1.56–1.24 (m, 16H), 0.96–0.88 (m, 6H); ^{13}C NMR (125 MHz, $CDCl_3$): δ 14.6, 23.2, 25.6, 29.5, 29.8, 32.3, 35.0, 119.6, 120.8, 121.4, 121.5, 127.6, 128.3, 129.3, 129.8, 131.5, 147.0, 172.8; MS (m/z): 536.1, 410.0, 284.2; IR (cm^{-1}): 2933, 2857, 1755, 1598, 1502, 1133, 1108, 799, 764; Calc'd for $C_{36}H_{40}O_4$ (M^+), 536.2927. Found, 536.2959.

2.5. Sample preparation

All samples were prepared under dim light conditions by dissolving the solid perylene analogues into a known volume of each solvent of interest (CCl_4, $CHCl_3$, CH_2Cl_2, pyridine, benzene, THF, toluene, and *tert*-butylbenzene). For example, perylene 3,9-dioctanoate **3** (4.1 mg, 7.64 × 10^{-6} mol) was weighed into a 20 mL scintillation vial on an analytical microbalance. Toluene (8.878 g, d = 0.8669 g/mL) was added to give a 7.5 × 10^{-4} M solution of **3**. A small volume of this initial solution (0.136 mL) was diluted in toluene (8.720 g) in a second 20 mL vial to give a final stock solution concentration of 1.0 × 10^{-5} M. The initial solution of dimethyl ether **1** was much more diluted than that of **2** and **3** due to the relative insolubility of **1**. Thus, 237.01 g of toluene was required to dissolve 2.4 mg of **1** (7.68 × 10^{-6} mol), giving an initial solution concentration of 2.8 × 10^{-5} M, which was further diluted to obtain the final stock solution with the 1.0 × 10^{-5} M concentration. For fluorescence experiments, the concentrations of the samples were adjusted so that the optical density of the excitation wavelength was less than 0.15 to ensure a uniform light distribution within the 1 cm optical pathlength of the quartz cells and to prevent nonlinear effects arising from changes in the geometry of the detection.

2.6. Absorption and calculation of the molar extinction coefficient (ε)

Absorption spectra were recorded in the 350–600 nm spectral range using an Evolution 300 UV–Vis dual beam spectrophotometer (Thermo-Scientific, Waltham, MA). Aromatic solvents (toluene and pyridine) gave interfering absorption signals in the UV region of the spectrum, and accordingly, the range of wavelengths scanned was reduced (380–600 nm). In addition, baseline absorbance spectra for all solvents were recorded and subtracted from the corresponding spectra of the perylene analogue solutions to obtain corrected absorption spectra. Molar extinction coefficients, ε, were obtained by progressively diluting a stock solution (10 μM) of each perylene analogue using the linear approximation of the Beer–Lambert law:

$$A = \varepsilon c l \quad (1)$$

where A is the optical density of the solution, c is the concentration of the perylene analogue, and l is the optical pathlength (1.0 cm in our case). The absorption spectra were recorded after each dilution using 3.5 ml quartz cells (NSG Precision Cells, Farmingdale, NY).

2.7. Fluorescence spectroscopy

Fluorescence spectra of **1**, **2**, and **3** in the various solvents were recorded using an AB2 double-monochromator fluorimeter (Thermo-Scientific, Waltham, MA). Samples were excited at wavelengths corresponding to the absorption peaks of the respective perylene analogues. For each excitation wavelength, fluorescence spectra were recorded from λ_{ex} +5–600 nm, in order to avoid the contribution of stray-light from the light source.

2.8. Fluorescence decay

Fluorescence decay of various perylene analogues in the different solvents were recorded using a time-correlated single photon counting (TCSPC) [15] instrument (5000U, Horiba JobinYvon, Edison, NJ). The light source was a pulsed LED at 457 nm (NanoLED-457, Horiba JobinYvon, Edison NJ) with pulsewidth of 1 ns and repetition rate at 1 MHz. Decays were recorded at the emission maxima of the perylene analogues ($\lambda_{em}^{max} \pm 4$ nm).

3. Data analysis

3.1. Transition dipole moment

An estimate of the magnitude of the dipole at the excited state, which indicates charge separation, was studied using the Lippert–Mataga method [16,17] which predicts a linear relationship between the Stoke shift and the function:

$$\Delta f = \frac{\delta - 1}{2\delta + 1} - \frac{n^2 - 1}{2n^2 + 1} \tag{2}$$

where δ is the dielectric constant of the solvent and n its index of refraction. The slope of the linear relation is proportional to the square of the change of dipole moment between the ground and the excited state of the chromophore, $\Delta\mu$.

3.2. Fluorescence decay

Analysis of fluorescence decay data was performed using the software DAS6.2 (JobinYvon, Edison, NJ). The analysis is carried out by assuming that the experimental decay profile is the convolution between the instrumental response function and the true fluorescence assumed to be a sum of exponentials according to

$$I(t) = \sum_i \alpha_i e^{-\frac{t}{\tau_i}} \tag{3}$$

with α_i being the relative amplitude of the component with lifetime τ_i. These parameters are retrieved by an algorithm that uses a Marquardt algorithm to fit the experimental decay with the convolution between $I(t)$ and the experimentally recorded instrument response function (often referred to as the profile of the pulsed source). The fitting algorithm varies the values of α_i and τ_i and the quality of the fitting is judged by the value of the reduced χ^2, the visual inspection and the autocorrelation of the residuals. The lifetime data includes only fittings that yielded a value of $1 < \chi^2 < 1.40$, and a Durbin–Watson factor in the 1.8–2.0 range [18].

3.3. Calculation of fluorescence quantum yield (Φ_f)

Fluorescence quantum yields were calculated using two different methods.

(1) The Strickler–Berg method [19] calculates Φ_f as the ratio between the fluorescence lifetime, τ_f, determined experimentally with TCSPC experiments (equation (3)), and the radiative lifetime, τ_R (derived from the absorption and emission spectra [19]):

$$\Phi_f = \frac{\tau_f}{\tau_R} \tag{4}$$

(2) The direct method estimates Φ_f by comparison with the emission of a reference of known fluorescence quantum yield [15] (in this case unsubstituted perylene [20]):

$$\Phi_f = \Phi_R \frac{I_f}{I_R} \frac{n_f^2}{n_R^2} \tag{5}$$

where Φ_R is the fluorescence quantum yield of the reference, I is the fluorescence intensity calculated as the area of the fluorescence spectrum after correction for the instrumental response and normalization for the optical density at the excitation wavelength [15], and n is the refractive index of the solvent.

The use of both methods enabled us to estimate interactions with solvents and changes in the excited state geometry, since in both these cases the Strickler–Berg method would fail to predict the correct quantum efficiency [15] and would yield a value of Φ_f different from that calculated by the direct method.

4. Results and discussion

4.1. Absorption spectroscopy

The UV–Vis spectra of **1**, **2**, and **3** in different solvents showed the typical vibronic structure of perylenes [21] (Fig. 1 and Supplemental Information). Analysis of the spectra indicated a separation of the vibrational levels of 0.17 ± 0.01 eV common to all the analogues in all solvents. This energy separation is in agreement with the perylene ring modes and indicates negligible effects of the substituents [12,22]. The analysis of the ratio between the three major vibronic peaks reveals that the $0 \leftarrow 0$, $1 \leftarrow 0$, and $2 \leftarrow 0$ transitions are not affected by solvents or concentrations (in the range of dilution of our experiments). The ratio of the intensity for the $0 \leftarrow 0/1 \leftarrow 0$ transition remains at 1.27 ± 0.02 and that for the $0 \leftarrow 0/2 \leftarrow 0$ transition remains at 2.8 ± 0.2 (this smaller peak is more affected by noise). This is an indication of negligible effects of the solvents as expected from the Onsager's reaction field function which is dominated by fast electronic polarization. Consequently, the spectra do not reveal a correlation between the position of the peaks and the polarity of the solvent (δ, or n of the solvent) [13]. However, two noticeable interactions among compounds and solvents were observed: (i) in all solvents, the absorption spectrum of **3** is significantly blue-shifted (11–16 nm; Table 1) with respect to both **1** and **2**, and (ii) the spectra of all compounds in pyridine are red-shifted (~3–5 nm) compared to those in all other non-polar solvents.

The molar extinction coefficients, ε, for various perylene analogues in different solvents were established (Fig. 2). The values of ε at the longest absorption maxima are summarized in Table 1. Once again there is no clear correlation between the values of the extinction coefficients and the polarity of the solvent, however it is worth noting that: (i) ε is significantly smaller for **1** than that for **2**

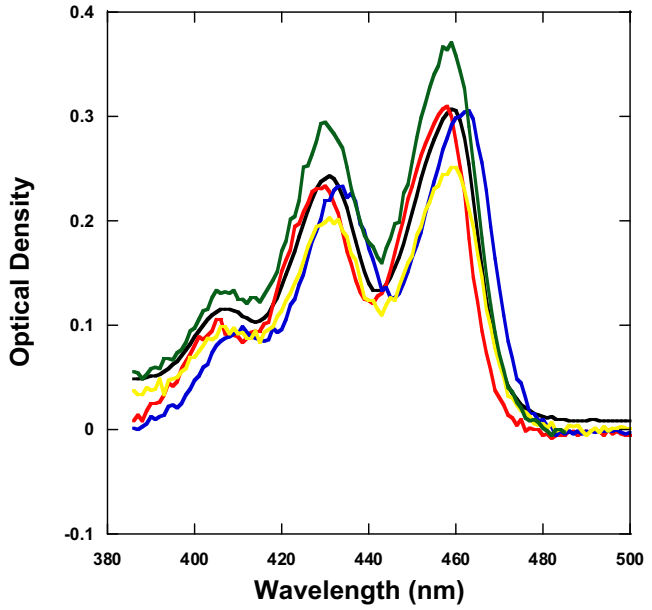

Fig. 1. Visible absorption spectra of **1** in various solvents [toluene (black), THF (red), pyridine (blue), $CHCl_3$ (yellow), and CH_2Cl_2 (green)]. (For interpretation of the references to colour in this figure legend, the reader is referred to the web version of this article).

and **3** in all solvents tested, (ii) the smallest value of ε among all the compounds is that of **1** in chloroform and it is much smaller than the smallest ε of either **2** or **3** in any solvent (at least 1.6 times smaller; Table 1), (iii) ε_{CCl_4} is smallest for **2** while ε_{CHCl_3} is the smallest for the other two compounds, and (iv) among chlorinated solvents, $\varepsilon_{CH_2Cl_2}$ shows the largest value for all three compounds.

4.2. Fluorescence spectroscopy

Emission spectra of **1**, **2**, and **3** recorded at different excitation wavelengths showed several important features. As was the case for the absorption, spectra of **3** are substantially blue-shifted compared to those of the other two analogues. The emission spectra of all three compounds are not affected by the excitation wavelength and maintain the same vibronic structure as representatively shown by the absorption and emission spectra of **2** in Fig. 3A and B. The position of the emission maxima do not strictly correlate with the dielectric properties of the solvent, which is typical for weak interactions between solvents and chromophores, however the fluorescence of **1** and **2** in pyridine is red-shifted (~3–4 nm) with respect to the other solvents, which is consistent with the red-shift shown in the absorption spectra under similar conditions (Supplemental Information).

The Stokes shifts calculated from absorption and emission spectra are summarized in Table 2. They show a weak correlation with the dielectric properties of the solvents. On average **1** exhibited the smaller Stokes shift across the various solvents (368 ± 40 cm^{-1} for **1** vs. 397 ± 60 cm^{-1} for **2**) while **3** showed the largest Stokes shift in every solvent (456 ± 29 cm^{-1}). An attempt at the Lippert–Mataga plots (data not shown) yielded scattered plots confirming a very small value of $\Delta\mu$ for all three perylenes **1**–**3**. At the same time the values of the Stokes shift (e.g., in pyridine) suggest specific interactions between some of the solvents and the perylene analogues.

4.3. Fluorescence decay

Fluorescence decay experiments of **1**–**3** show that in all solvents (except CCl_4), the decay of emission is monoexponential and does not depend on the emission wavelength (as represented by the fluorescence decay of **1** in Fig. 4A). The measured fluorescence lifetimes of **1**–**3** are shorter than the ones obtained for the unsubstituted perylene in the same solvents (Table 3). There is no clear correlation between the fluorescence decay and the dielectric properties of the solvents (Table 3). Nevertheless, there is a correlation between the order of chlorination of the solvent and the fluorescence lifetime of all the chromophores (Fig. 4B). Accordingly, chlorinated solvents are the only ones that require a second component to significantly increase the quality of decay fitting. This second component is typically at the resolution limit of our instrumentation (<300 ps) and is very small (<5%) in $CHCl_2$ and $CHCl_3$. However the relative contribution of this picosecond component increases with increasing number of chlorine atoms in the solvent molecule and becomes prevalent (>90%) in CCl_4 (i.e., red curve in Fig. 4B). The remaining nanosecond component of **3** (tail end of red curve in Fig. 4B) is slightly longer-lived than those of **1** and **2** (except in pyridine; Table 3).

4.4. Fluorescence quantum yield (Φ_f)

The values of fluorescence quantum yields, Φ_f, were estimated by two different methods using equation (4) [15,19] and equation (5) [15]. In most solvents **1**, **2**, and **3** yield a smaller quantum yield than that of unsubstituted perylene [20] and many other perylene derivatives for which Φ_f is close to unity [23,24].

The diester **3** and the dioctyl ether **2** generally show a large Φ_f (>0.75; Table 4). Compound **1** has a significantly smaller value of Φ_f (Table 4). Comparison of Φ_f values calculated with the two methods reveals a consistent discrepancy where, apart from few exceptions, the quantum yield provided by the Strickler–Berg method is smaller than the one obtained by the direct method. The discrepancy is particularly evident in chlorinated solvents and in pyridine. Another trend seen among chlorinated solvents is that the value of

Table 1
Values of the molar extinction coefficients (ε) of the perylene analogues in select solvents.

Solvent	ε (M^{-1} cm^{-1})[a,b]			Solvent dipole moment[c]
	1	2	3	
Carbon Tetrachloride	2.62×10^4 (460)	3.15×10^4 (462)	3.36×10^4 (448)	0.00
Toluene	2.68×10^4 (459)	3.70×10^4 (462)	3.56×10^4 (448)	0.37
Chloroform	1.98×10^4 (459)	3.41×10^4 (462)	3.35×10^4 (446)	1.04
Dichloromethane	2.98×10^4 (459)	3.92×10^4 (461)	4.03×10^4 (445)	1.60
THF	3.08×10^4 (458)	3.76×10^4 (460)	3.42×10^4 (445)	1.75
Pyridine	3.69×10^4 (463)	3.91×10^4 (464)	3.45×10^4 (449)	2.20

[a] The given ε values are for those of the largest absorption maximum in M^{-1} cm^{-1}.
[b] Values in brackets are the corresponding wavelength of the maximum in nm.
[c] Values are in Debye (From CRC Handbook of Chemistry and Physics: 86th Edition; David R. Lide, Ed.; CRC Press: Boca Raton, FL, 2005).

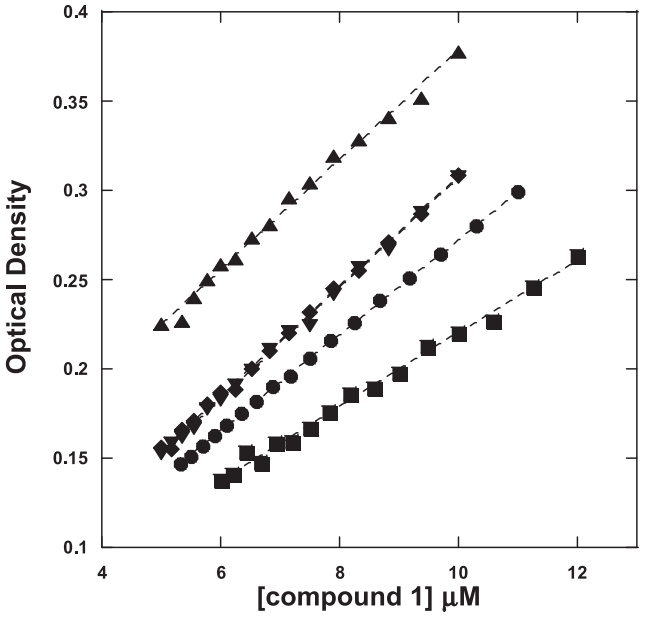

Fig. 2. Linear trend of the optical density of **1** in various solvents [(●) toluene, (■) $CHCl_3$, (▲) CH_2Cl_2, (◆) THF, and (▼) pyridine].

Φ_f decreases dramatically with the increasing number of chlorine atoms in the solvent molecule. In CCl_4 the longer nanosecond component produces a larger quantum yield from the Strickler–-Berg method, however because such component has a very small relative contribution it creates the large discrepancy (Table 4) since the direct method accounts for the missing fluorescence due to quenching (see below) which is not considered by the Strickler–Berg method.

Taken altogether, absorption and emission spectra of **1**–**3** (Figs. 1 and 2) are consistent with those of the other perylenes in solution [9,22,25,26], which are dominated by the 0 ← 0, 1 ← 0, and 2 ← 0 vibronic levels of the $\pi \rightarrow \pi^*$ transitions. The linearity of the optical density (Fig. 2 and Supplemental Information) in the range of the investigated concentrations confirms that all perylene analogues are monomeric, and enabled us to retrieve the corresponding value of ε. The values obtained are comparable to those obtained for the unsubstituted perylene and other perylene derivatives [13,24] with the exception of compound **1**. The smaller value of ε for the dimethoxy-analogue **1** is consistent with the results observed in other dimethoxy-substituted polycyclic aromatic hydrocarbons (PAH) [27], however a mechanistic explanation for this effect would require either computational characterization of HOMO–LUMO electronic configurations or Density Functional Theory calculations [28,29].

Inspection of the data reveals that, compared to **1** and **2**, the spectra of compound **3** are significantly shifted to higher energies (closer to the values for unsubstituted perylene [15,20]). This effect could be due to the weakly electron-withdrawing nature of the acyloxy substituents of **3** or to the $n \rightarrow \pi^*$ contribution to the spectrum due to the carbonyl group [30]. The substituents in **1** and **2**, in fact, provide electron donating properties that contribute to the energy stabilization of the π^* orbital [31,32]. From the spectra, such energy stabilization can be estimated, on average, to be 0.085 ± 0.006 eV with respect to **3**.

The scattered Lippert–Mataga plots are an indication of an extremely small value of $\Delta\mu$ (<2 Debye [13]) for all three perylenes **1**–**3**. The photophysical properties suggest that the small value of $\Delta\mu$ is due to the symmetrical nature of the compounds rather than the presence of particular groups or lack of interaction with the solvent. In fact, the larger Stokes shift of **3** (with respect to **1** and **2**) and the red-shifts of all three compounds in pyridine clearly indicate solvent interactions. Moreover, the large change in ε for each chromophore in different solvents indicates that the interaction with the solvent is strong enough to affect the cross section of the absorption (probably by distorting the overlap between HOMO and LUMO).

The carbonyl group in **3** may cause its significantly larger Stokes shift compared to that of **2** in all solvents. The relatively high Stokes shifts in pyridine suggest that the interaction of π-system of the solvents may also play a role in relaxation. All three perylene analogues show red-shifted absorption and fluorescence spectra (Figs. 1 and 3B, and Supplemental Information) in pyridine. We suggest that this is due to π-stacking between pyridine molecules and the perylene nucleus. Similar π-stacking would in principle be

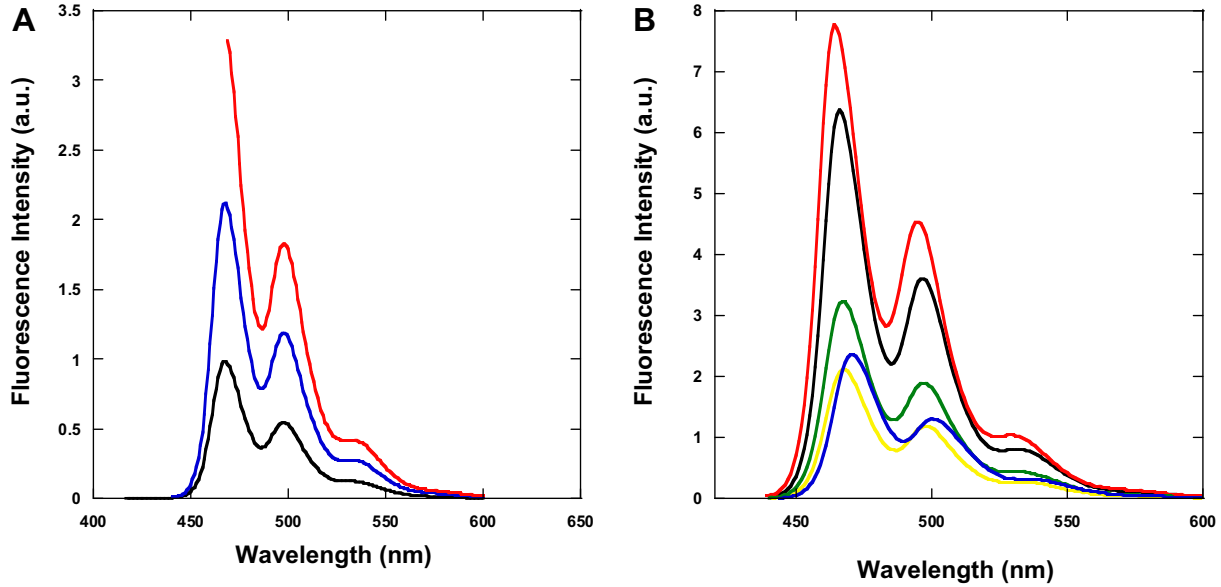

Fig. 3. (A) Emission spectra of **2** in toluene at excitation wavelengths corresponding to the vibronic peaks in absorption spectra [λ_{ex} = 411 nm (black), λ_{ex} = 434 nm (blue), and λ_{ex} = 462 nm (red)]. (B) Emission spectra of **2** (excited at the lower absorption peak) in various solvents [toluene (black), THF (red), pyridine (blue), $CHCl_3$ (yellow), and CH_2Cl_2 (green)]. (For interpretation of the references to colour in this figure legend, the reader is referred to the web version of this article).

Table 2
Stokes shift for the perylene analogues in various solvents.

Solvent	Stokes shift (cm^{-1})		
	1	2	3
Carbon tetrachloride	371	414	439
Toluene	327	277	439
Chloroform	418	414	492
Dichloromethane	373	415	494
THF	282	373	446
Pyridine	321	455	486
Benzene	418	414	582
tert-Butylbenzene	329	370	585

Table 3
Fluorescence lifetime and relative amplitude of nanosecond decay component of perylene analogues in different organic solvents.

Solvent	Fluorescence lifetime (ns)			
	1	2	3	perylene
Carbon Tetrachloride	3.65 ± 0.04	3.82 ± 0.05	3.89 ± 0.04	4.89 ± 0.04
Toluene	3.60 ± 0.04	3.65 ± 0.05	3.72 ± 0.07	4.72 ± 0.07
Chloroform	3.89 ± 0.05	3.77 ± 0.04	4.16 ± 0.06	5.12 ± 0.06
Dichloromethane	4.33 ± 0.06	4.17 ± 0.06	4.34 ± 0.05	5.36 ± 0.05
THF	3.95 ± 0.05	3.88 ± 0.03	4.35 ± 0.04	4.92 ± 0.04
Pyridine	4.02 ± 0.05	4.01 ± 0.05	3.88 ± 0.03	5.32 ± 0.03

possible with toluene but its methyl group may prevent a more complete overlap of the solvent and solute aromatic nuclei. This interpretation is supported by data obtained in benzene and *tert*-butylbenzene. Although absorption spectra are only slightly red-shifted in benzene compared to that in *tert*-butylbenzene (<2 nm; Fig. 5A and Supplemental Information), the fluorescence spectra show a more substantial red-shift (>4 nm; Fig. 5B). These results indicate that the π-stacking is stabilized at the excited state of electron rich **1** and **2** (by the electron donation of the substituents to the π-system), which indeed, lowers the interaction energy and shifts the emission wavelength, but not in **3** (Fig. 5C and Supplemental Information) where the substituents on the perylene moiety do not donate an electron to the π-system. For compound **3** and in most solvents for **1** and **2**, the spectral shifts are likely determined by the electronic polarizability of the compounds at the ground and excited states [9].

The rest of the results show that there is no relationship between relaxation and solvent polarity (*cf.*, the values in THF) however they point to effects produced by chlorinated solvents (generally, in the order of $CH_2Cl_2 > CHCl_3 > CCl_4$). These will be addressed in future studies.

The values of Φ_f (Table 4) measured with the direct method, using unsubstituted perylene as reference, show that the diester **3** has, on average, the highest efficiency (>0.8) closer to the value reported for unsubstituted perylene [25]. Compounds **1** and **2** have significantly lower quantum efficiencies. This is consistent with an enhanced intramolecular electron transfer mechanism to the π-system in compounds **1** and **2**.

The inadequacy of the Strickler–Berg method reflected by the discrepancy of the Φ_f values in Table 4 can occur when (1) there is a substantial change in the geometry of the molecule at the excited state or (2) when there is a strong interaction with the solvent. Both cases can be made in our system. Large rearrangement of the geometry of the molecule at the excited state may occur, however, intramolecular electron transfer to the π-system implies an electronic rearrangement that could have effects equivalent to geometric rearrangements. At the same time parameters in Tables 3 and 4 for the three compounds investigated show likely interactions with the solvents. Such interaction is evident in pyridine and in the three chlorinated solvents and this explains the large difference between the values of Φ_f predicted with the Strickler–Berg method and the ones measured directly.

For all compounds the Φ_f in chlorinated solvents is lower than in all other solvents and its value decreases with the increasing content of chlorine atoms. This effect is consistent with the fluorescence quenching properties of chlorine atoms. These manifest via strong spin–orbit interactions with the π^* orbital in static as well as collisional quenching as proven by the decrease in fluorescence lifetime and the presence of a predominant fast decay component (Fig. 4B, Table 3, Supplemental Information) in CCl_4. The strong interactions with chlorinated compounds also produce photochemical reactions (not observed with the other solvents) that are being investigated at the moment.

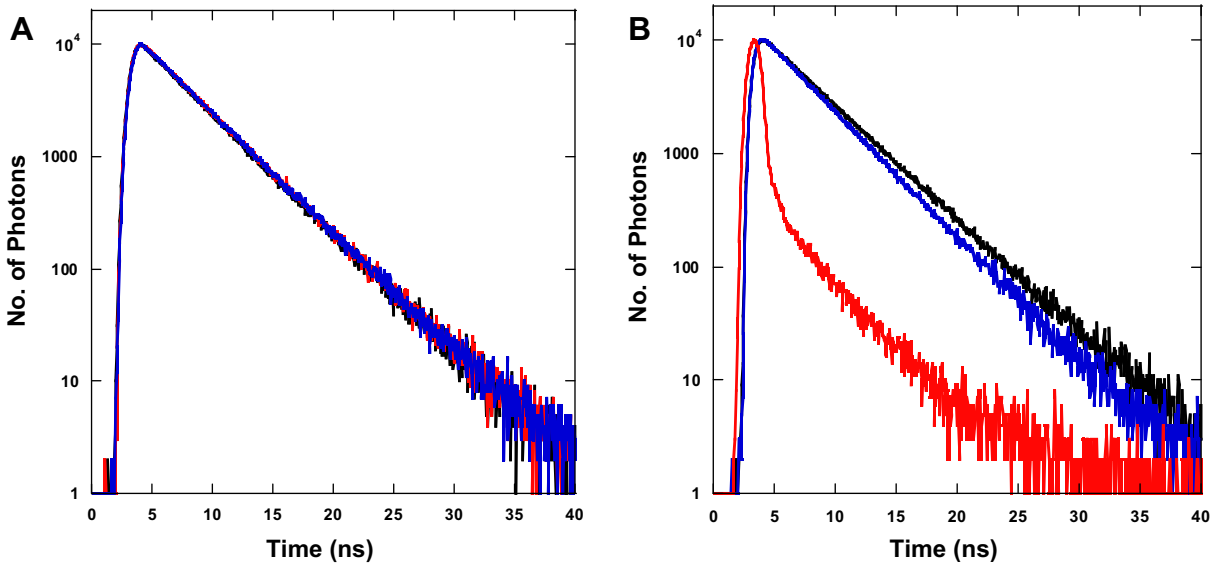

Fig. 4. (A) Fluorescence decay of **1** in toluene (black), THF (red), and pyridine (blue). (B) Fluorescence decay of **1** (black), **2** (blue), and **3** (red) in CCl_4. (For interpretation of the references to colour in this figure legend, the reader is referred to the web version of this article).

Table 4
Fluorescence quantum yields (Φ_f) of the perylene analogues in selective solvents.

Solvent	Fluorescence quantum yields (Φ_f)[a,b]		
	1	2	3
Carbon Tetrachloride	0.58 (0.05)	0.60 (0.08)	0.64 (0.06)
Toluene	0.76 (0.76)	0.77 (0.90)	0.79 (0.97)
Chloroform	0.76 (0.82)	0.74 (0.69)	0.81 (0.91)
Dichloromethane	0.81 (0.94)	0.78 (0.81)	0.81 (0.80)
THF	0.80 (0.88)	0.80 (0.94)	0.88 (0.97)
Pyridine	0.76 (0.90)	0.76 (0.90)	0.97 (0.93)

[a] Calculated according to the Strickler–Berg method using equation (4).
[b] Values in parenthesis are calculated according to the direct method using equation (5).

In conclusion we have characterized several important photophysical parameters of a series of novel perylene compounds (**1**–**3**) in various solvents. These values can be used to develop studies on the potential properties of these compounds as fluorescent molecules as well as organic semiconductors. These perylene derivatives interact differently with various solvents and, in addition, intramolecular electron transfer likely occurs in compound **1** and **2**. This evidence grants further investigation of the excited state properties of these compounds and their reactivity to explore their use as photoactive molecules and fluorescent tags.

Acknowledgement

This work was in part funded by a seed grant from the Vice President for Research at the University of Texas at San Antonio, TX.

Appendix. Supplementary data

Supplementary data associated with this article can be found in the online version, at doi:10.1016/j.dyepig.2010.06.009.

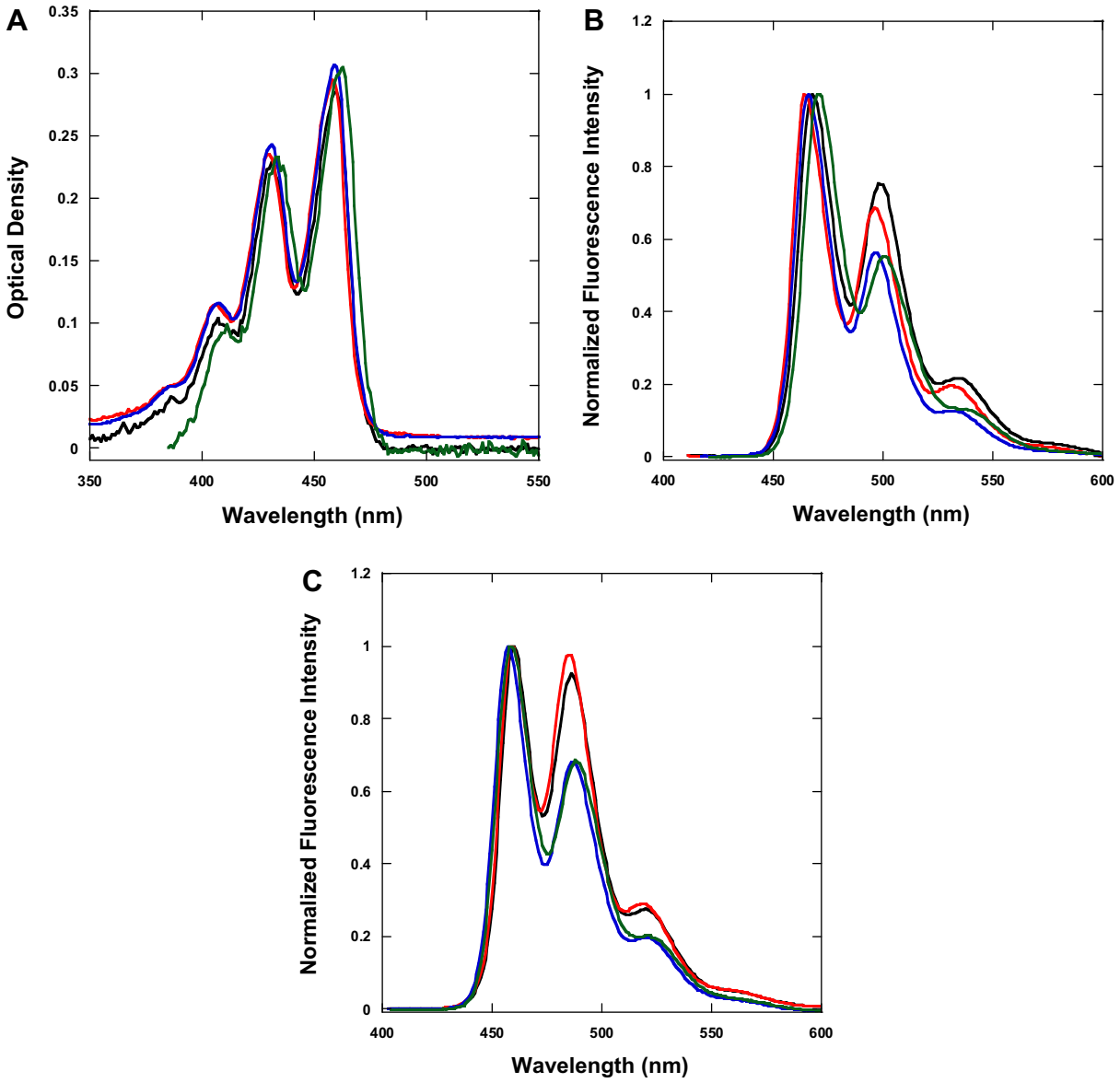

Fig. 5. (A) Visible absorption spectra of **1** in various aromatic solvents [benzene (black), *tert*-butylbenzene (red), pyridine (green), and toluene (blue)]. (B) Normalized fluorescence spectra of **1** in various aromatic solvents [benzene (black), *tert*-butylbenzene (red), pyridine (green), and toluene (blue)]. (C) Normalized fluorescence spectra of **3** in various aromatic solvents [benzene (black), *tert*-butylbenzene (red), pyridine (green), and toluene (blue)]. (For interpretation of the references to colour in this figure legend, the reader is referred to the web version of this article).

References

[1] Langhals H. Cyclic carboxylic imide structures as structure elements of high stability. Novel developments in perylene dye chemistry. Heterocycles 1995;40:477–500.

[2] Takahashi M, Morimoto H, Miyake K, Yamashita M, Kawai H, Sei Y, et al. Evaluation of energy transfer in perylene-cored anthracene dendrimers. Chem Commun; 2006:3084–6.

[3] Julien C, Débarre A, Nutarelli D, Richard A, Tchénio P. Single molecule study of perylene orange photobleaching in thin sol–gel films. J Phys Chem B 2005;109:23145–53.

[4] Feng L, Chen Z. 2-Mercaptobenzothiazole benzoates as highly sensitive fluorescent enhancement chemosensors for transition metal ions. Sens Actuators B Chem. 2007;122:600–4.

[5] Flors C, Oesterling I, Schnitzler T, Fron E, Schweitzer G, Sliwa M, et al. Energy and electron transfer in ethynylene bridged perylene diimide multichromophores. J Phys Chem C 2007;111:4861–70.

[6] Banerji N, Angulo G, Barabanov I, Vauthey E. Intramolecular charge-transfer dynamics in covalently linked perylene-dimethylaniline and cyanoperylene-dimethylaniline. J Phys Chem A 2008;112:9665–74.

[7] Asir S, Demir AS, Icil I. The synthesis of novel, unsymmetrically substituted, chiral naphthalene and perylene diimides: photophysical, electrochemical, chiroptical and intramolecular charge transfer properties. Dyes Pigm 2010;84:1–13.

[8] Würthner F. Perylene bisimide dyes as versatile building blocks for functional supramolecular architectures. Chem Commun; 2004:1564–79.

[9] Heinz H, Suter UW, Leontidis E. Simple and accurate computations of solvatochromic shifts in π–π^* transitions of aromatic chromophores. J Am Chem Soc 2001;123:11229–36.

[10] Joblin C, Salama F, Allamandola L. Absorption and emission spectroscopy of perylene ($C_{20}H_{12}$) isolated in Ne, Ar and N_2 matrices. J Chem Phys 1999; 110:7287–97.

[11] Benshafrut R, Hoffman RE, Rabinovitz M, MullenAn K. Unusual charge umpolung: synthesis of the bay region diketone 2,3:10,11-dibenzoperylene-1,12-dione. J Org Chem 1999;64:644–7.

[12] Vragovic I, Scholz R, Schreiber M. Model calculation of the optical properties of 3,4,9,10-perylene-tetracarboxylic-dianhydride (PTCDA) thin films. Europhys Lett 2002;57:288–94.

[13] Zoon PD, Brouwer AM. Paradoxical solvent effects on the absorption and emission spectra of amino-substituted perylene monoimides. ChemPhysChem 2005;6:1574–80.

[14] Penick MA, Mahindaratne MP, Gutierrez RD, Smith TD, Tiekink ER, Negrete GR. Tandem Friedel-Crafts annulation to novel perylene analogues. J Org Chem 2008;73:6378–81.

[15] Lakowicz JR. Principles of fluorescence spectroscopy. 3rd ed. New York: Springer; 2006.

[16] Lippert E. Dipole moment and electronic structure of excited molecules. Z Naturforsch A Phys Sci 1955;10:541–4.

[17] Mataga N, Kaifu Y, Koizumi M. Solvent effects upon fluorescence spectra and the dipole moments of excited molecules. Bull Chem Soc Jpn 1956;29: 465–70.

[18] Harvey BJ, Bell E, Brancaleon L. A tryptophan rotamer located in a polar environment probes pH-dependent conformational changes in bovine beta-lactoglobulin A. J Phys Chem B 2007;111:2610–20.

[19] Strickler SJ, Berg RA. Relationship between absorption intensity and fluorescence lifetime of molecules. J Chem Phys 1962;37:814–22.

[20] Du H, Fuh RA, Li J, Corkan A, Lindsey JS. PhotochemCAD: a computer-aided design and research tool in photochemistry. Photochem Photobiol 1998; 68:141–2.

[21] Müller S, Müllen K. Facile synthetic approach to novel core-extended perylene carboximide dyes. Chem Commun; 2005:4045–6.

[22] Jiang Y, Blanchard GJ. Vibrational population relaxation of perylene in *n*-alkanes. The role of solvent local structure in long-range vibrational energy transfer. J Phys Chem 1994;98:9411–6.

[23] Do JY, Kim BG, Kwon JY, Shin WS, Jin S-H, Kim Y-I. Soluble asymmetric perylene derivatives for organic solar cells. Macromol Symp 2007;249–250:461–5.

[24] Zhao G-J, Han K-L. Excited state electronic structures and photochemistry of heterocyclic annulated perylene (HAP) materials tuned by heteroatoms: S, Se, N, O, C, Si, and B. J Phys Chem A; 2009.

[25] Birks JB. Photophysics of aromatic molecules. Wiley & Sons; 1970.

[26] Katoh R, Sinha S, Murata S, Tachiya M. Origin of the stabilization energy of perylene excimer as studied by fluorescence and near-IR transient absorption spectroscopy. J Photochem Photobiol A 2001;145:23–34.

[27] Seixas de Melo JS, Rondo R, Burrows HD, Melo MJ, Navaratnam S, Edge R, et al. Spectral and photophysical studies of substituted Indigo derivatives in their keto forms. ChemPhysChem. 2006;7:2303–11.

[28] Parac M, Grimme SA. TDDFT study of the lowest excitation energies of polycyclic aromatic hydrocarbons. Chem Phys 2003;292:11–21.

[29] Kang SJ, Yi Y, Cho K, Jeong K, Yoo K-H, Whang CN. Electronic structure of perylene on Au studied by ultraviolet photoelectron spectroscopy and density functional theory. Synth Metals 2005;151:120–3.

[30] Sanchez-Garcia E, Doerr M, Thiel W. QM/MM study of the absorption spectra of DsRed.M1 chromophores. J Comput Chem Dec 2009;14 [Eprint ahead].

[31] Miller SR, Krasutsky S, Kiprof P. Stability of carboxonium ions. J Mol Struct (Theochem) 2004;674:43–7.

[32] Baird NC. π-Electron hyperconjugation in organic molecules and ions. Theor Chim Acta 1970;16:239–42.